
Proc. XXXVII International School of Semiconducting Compounds, Jaszowiec 2008

Raman Scattering from ZnO(Fe) Nanoparticles

N. ROMČEVIĆ^{a,*}, R. KOSTIĆ^a, M. ROMČEVIĆ^a, B. HADŽIĆ^a,
I. KURLISZYN-KUDELSKA^b, W. DOBROWOLSKI^b,
U. NARKIEWICZ^c AND D. SIBERA^c

^aInstitute of Physics, Pregrevica 118, 11080 Belgrade, Serbia

^bInstitute of Physics, Polish Academy of Sciences
al. Lotników 32/46, 02-668 Warszawa, Poland

^cSzczecin University of Technology
Institute of Chemical and Environment Engineering
Pułaskiego 10, 70-322 Szczecin, Poland

Nanocrystalline samples of ZnO(Fe) were synthesized by wet chemical method. Samples were characterized by X-ray diffraction to determine composition of the samples (ZnO, Fe₂O₃, ZnFe₂O₄) and the mean crystalline size (8–52 nm). In this paper we report the experimental spectra of the Raman scattering (from 200 to 1600 cm⁻¹). Main characteristics of experimental Raman spectrum in 200 to 1600 cm⁻¹ spectral region are: sharp peak at 436 cm⁻¹ and broad two-phonon structure at ≈ 1150 cm⁻¹, typical of ZnO; broad structure below 700 cm⁻¹ that has different position and shape in case of ZnFe₂O₄ or Fe₂O₃ nanoparticles.

PACS numbers: 63.20.-e, 78.30.Fs, 78.67.-n

1. Introduction

Recently, a continued interest in the synthesis and properties of nanoscale inorganic materials has been observed. Semiconductor nanocrystals have been of much interest over two decades because of their unique physical properties resulting from modification of the electronic states due to the confinement effect. Currently, nanostructures made of ZnO have attracted significant attention owing to their proposed applications in low-voltage and short-wavelength electro-optical devices, transparent ultraviolet protection films, and spintronic devices [1, 2].

A considerable attention has recently been devoted to high temperature ferromagnetism observed in transition metal doped oxides. Particularly ZnO has been identified as a promising host semiconductor material, exhibiting ferromag-

*corresponding author; e-mail: romcevi@phy.bg.ac.yu

netism when doped with most of the transition metals — V, Cr, Fe, Co, Ni [3]. However, the origin of ferromagnetic behavior is not very well known in these compounds. Recently, it was shown that the ferromagnetism in these materials can be induced by inclusions of nanoscale oxides of transition metals [4] and/or nanoparticles containing a large concentration of magnetic ions [5]. Novel methods enabling a control of nanoassembling of magnetic nanocrystals in nonconducting matrices as well as functionalities specific to such systems were described [5].

The samples were synthesized with the use of the wet chemical method. First, the mixture of iron and zinc hydroxides was obtained by addition of an ammonia solution to the 20% solution of proper amount of $\text{Zn}(\text{NO}_3)\cdot 6\text{H}_2\text{O}$ and $\text{Fe}(\text{NO}_3)\cdot 4\text{H}_2\text{O}$ in water. Next, the obtained hydroxides were filtered, dried and calcined at 300°C during one hour. A series of samples containing from 5 to 95% of Fe_2O_3 was obtained. The phase composition of the samples was determined by X-ray diffraction (XRD) ($\text{Co } K_\alpha$ radiation, X'Pert Philips). The crystalline phases of hexagonal ZnO, rhombohedral Fe_2O_3 and cubic ZnFe_2O_4 were identified as presented in [6].

XRD data allowed to determine a mean crystallite size in prepared samples with the use of Scherrer's formula [7]. The mean crystallite size a of these phases are given in Table 1 in Ref. [6].

In this work we present investigation of two samples. First sample is assigned as $(\text{ZnO})_{0.95}(\text{Fe}_2\text{O}_3)_{0.05}$ (sample contains 5 wt.% of Fe_2O_3), where crystalline phase of ZnFe_2O_4 is identified. Mean crystallite size is $a = 10$ nm. Second sample is assigned as DS90Fe10Zn (sample contains 90 wt.% of Fe_2O_3) where crystallite of Fe_2O_3 is identified with mean crystallite size $a = 24$ nm. No other crystal phases are observed in these samples.

XRD measurements did not reveal presence of ZnO phase in these samples. It is interesting that for the samples with lower concentration of Fe_2O_3 (up to 20 wt.% of Fe_2O_3) excitonic lines from ZnO are observed. In some samples, for instance sample containing 40 wt.% of Fe_2O_3 , crystallites of ZnO and ZnFe_2O_4 are identified [6].

2. Results and discussion

The micro-Raman spectra were taken in the backscattering configuration and analyzed using Jobin Yvon T64000 spectrometer, equipped with nitrogen cooled charge-coupled-device detector. As excitation source we used the 514.5 nm line of an Ar-iron laser. The measurements were performed at different laser power.

In Fig. 1 the Raman spectra of nanocrystalline ZnO doped with 5 wt.% of Fe_2O_3 assigned as $(\text{ZnO})_{0.95}(\text{Fe}_2\text{O}_3)_{0.05}$ are presented. Only nanoparticles of ZnFe_2O_4 are registered by XRD.

We will start analysis of spectrum in Fig. 1 with brief report about structure and vibrational properties of potentially present materials in sample. Vibrational properties of bulk material are crucial for understanding vibrational properties of

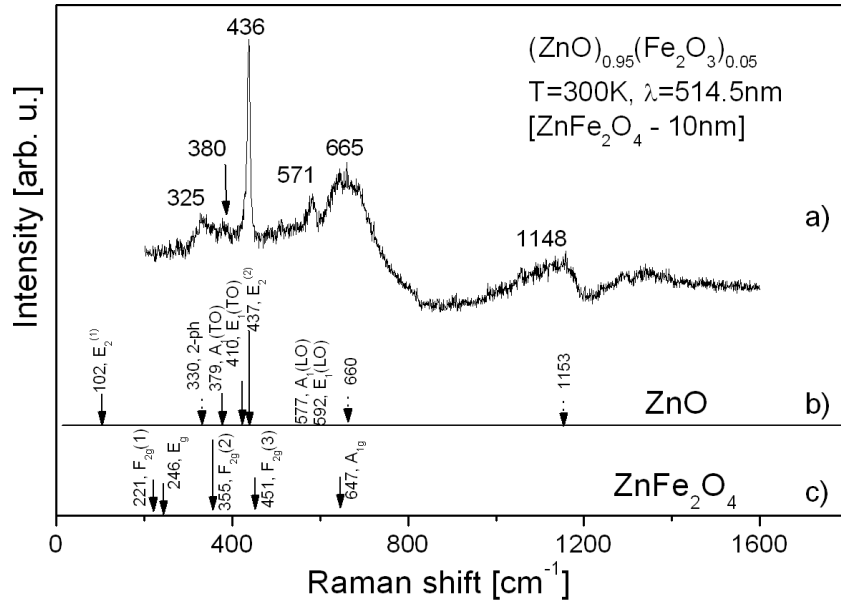


Fig. 1. Raman spectra of nanocrystalline ZnO doped with 5 wt.% of Fe_2O_3 assigned as $(\text{ZnO})_{0.95}(\text{Fe}_2\text{O}_3)_{0.05}$.

small particles. As consequence of miniaturization, we expect bulk modes to be shifted and broadened.

Basic material in this research is ZnO. ZnO is a semiconductor with a wurtzite crystal structure. This hexagonal structure belongs to the space group C_{6v}^4 , with two formula units per primitive cell, where all atoms occupy C_{3v} sites. The optical phonons at the center of the Brillouin zone belong to the following irreducible representations: $\Gamma_{\text{opt}} = A_1 + 2B_1 + E_1 + 2E_2$. Modes of symmetry A_1 , E_1 and E_2 are Raman active, and A_1 and E_1 are infrared active. B_1 are inactive (silent) modes. Both A_1 and E_1 are polar modes and split into transverse (TO) and longitudinal (LO) phonons with different frequencies due to macroscopic electric fields associated with the LO phonons. The short-range interatomic forces cause anisotropy. That is why A_1 and E_1 modes have different frequencies. As the electrostatic forces dominate the anisotropy in the short-range forces, the TO-LO splitting is larger than the A_1 - E_1 splitting. For the lattice vibration A_1 atoms move parallel to the c -axis and for E_1 perpendicular to c -axis. Two nonpolar Raman active modes, are often assigned as $E_2^{(1)}$ (low), and $E_2^{(2)}$ (high). All these modes have been reported in the Raman scattering spectra of bulk ZnO many times [8, 9]. Frequencies and assignation of the Raman active modes in ZnO are presented in the bottom of Fig. 1b. Solid lines indicate A_1 , E_1 and E_2 phonon modes in ZnO. Dashed lines mark multiphonon scattering at $\approx 330 \text{ cm}^{-1}$, $\approx 655 \text{ cm}^{-1}$ and $\approx 1153 \text{ cm}^{-1}$ (2LO).

ZnFe₂O₄ spinel has a cubic structure that belongs to the space group O_h^7 . Full unit cell contains eight formula units, and primitive cell contains two formula units. The optical phonons at Γ -point of the Brillouin zone belong to the following irreducible representations: $\Gamma_{\text{opt}} = A_{1g} + E_g + F_{1g} + 3F_{2g} + 2A_u + 2E_u + 4F_{1u} + 2F_{2u}$. There are five first-order active Raman modes: A_{1g} , E_g and $3F_{2g}$. Modes F_{1u} are infrared-active. In the cubic spinels, including ferrites, the modes above 600 cm^{-1} mostly correspond to the motion of oxygen atoms in tetrahedral AO₄ group. The other lower frequency modes represent the characteristic of the octahedral BO₆ sites. Frequencies [10] and assignments of Raman-active modes in ZnFe₂O₄ are presented in the bottom of Fig. 1c.

Let us dispute the fact that XRD does not evidence ZnO, sharp peak in our spectrum at 436 cm^{-1} is clearly $E_2^{(2)}$ mode of ZnO. Position is practically the same as in bulk material. Phonon dispersion relation, that corresponds to the $E_2^{(2)}$ mode in ZnO at the Γ point, does not show considerable dispersion. Therefore, even in ZnO nanoparticle spectra position of this mode is practically unchanged. The peak at $\approx 571 \text{ cm}^{-1}$ is identified as LO ZnO mode. Also structure at $\approx 1150 \text{ cm}^{-1}$ can be prescribed to multiphonon 2LO mode in ZnO. Wide and dominant structure centered at 665 cm^{-1} corresponds to vibrations in the tetrahedral AO₄ group. Materials like: Mn₃O₄, Fe₃O₄, Co₃O₄ have Raman active mode in interval $600\text{--}700 \text{ cm}^{-1}$. Even in bulk ZnFe₂O₄ the three most intensive Raman modes at 355 cm^{-1} , 451 cm^{-1} and 647 cm^{-1} exhibit broad characteristics. If there is any disorder of the Zn and Fe cations in the tetrahedral and octahedral sites, the vibrations related to the two types of cations at the same site may result in two separated first order Raman modes. If they are very close in frequency an overlapped broad peak should be observed.

The Raman spectrum in region below 400 cm^{-1} is superposition of characteristic frequencies of ZnO phase and spectrum of ZnFe₂O₄ nanoparticles. In bulk ZnFe₂O₄ mode at 355 cm^{-1} is strong and wide, and modes at 221 cm^{-1} and 246 cm^{-1} are weak. In ZnFe₂O₄ nanoparticles these modes are wider and contribute to high level of spectral curve.

In Fig. 2 the Raman spectra of nanocrystalline ZnO doped with 90 wt.% of Fe₂O₃ assigned as DS90Fe10Zn is presented. Only nanoparticles of Fe₂O₃ are registered by XRD.

We will give brief report about structure and vibrational properties of Fe₂O₃. Fe₂O₃ crystallize in the rhombohedral (trigonal) system with space group D_{3d}^6 . Primitive unit cell contains two formula units. The optical phonons at the Γ -point of the Brillouin zone belong to the following irreducible representations: $\Gamma = 2A_{1g} + 2A_{1u} + 3A_{2g} + 2A_{2u} + 5E_g + 4E_u$. $2A_{1g}$ and $5E_g$ are Raman active modes. $2A_{2u}$ and $4E_u$ modes are infrared active. Information about Fe₂O₃ Raman spectra are presented at the bottom of Fig. 2c [11–13]. In addition to these first order Raman spectra there is a very prominent peak at $\approx 1320 \text{ cm}^{-1}$. LO phonon situated at $\approx 660 \text{ cm}^{-1}$ is Raman forbidden. It can be activated, and become

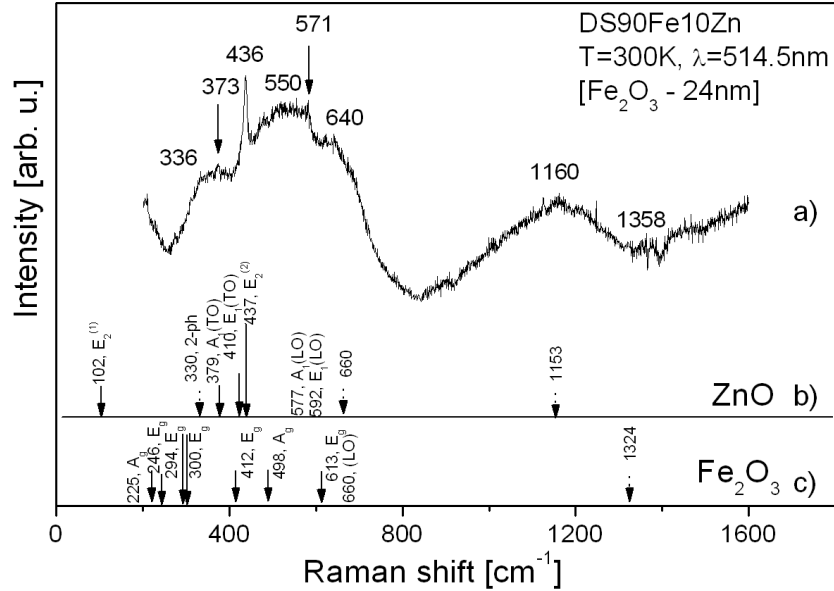


Fig. 2. Raman spectra of nanocrystalline ZnO doped with 90 wt.% of Fe₂O₃ assigned as DS90Fe10Zn.

visible, if symmetry rules are broken. The 2LO mode which is Raman allowed is seen in all the spectra. Strength of this mode is remarkable in case of resonance.

ZnO mode at 436 cm⁻¹, LO ZnO mode at ≈ 571 cm⁻¹ and ZnO multiphonon mode at ≈ 1160 cm⁻¹ can easily be identified. In spectral region below 400 cm⁻¹ there is a superposition of ZnO phase and Fe₂O₃ nanoparticles spectrum. Difference of spectra in Fig. 1 and Fig. 2, in region below 400 cm⁻¹ is a consequence of presence of ZnFe₂O₄ (Fig. 1) or Fe₂O₃ (Fig. 2) nanoparticles.

We present Raman spectra to be more sensitive to material composition than XRD measurements. On the basis of these data we cannot exclude possibility that both samples contain some other phases that are not included in this analysis.

3. Conclusion

Small amount (5 wt.%) of Fe₂O₃ at the beginning of the synthesis results in forming of ZnFe₂O₄ nanoparticles. Large amount (90 wt.%) of Fe₂O₃ at the beginning of the synthesis results in forming of Fe₂O₃ nanoparticles. Both samples also contain ZnO phase which is not registered by XRD, but is clearly seen in the Raman spectra.

Acknowledgments

This work was supported under the Agreement of Scientific Collaboration between Polish Academy of Sciences and Serbian Academy of Sciences and Arts.

The work in Serbia was supported by Serbian Ministry of Science (project 141028) and supported by Research Network WITNANO and Polish Ministry for Higher Education and Science.

References

- [1] Y. Chen, D.M. Bagnall, H. Koh, K. Park, K. Higara, Z. Zhu, T. Yao, *J. Appl. Phys.* **84**, 3912 (1988).
- [2] J. Nemeth, G. Rodriguez-Gattorno, A. Diaz, I. Dekany, *Langmuir* **20**, 2855 (2004).
- [3] J.M.D. Coey, M. Venkatesan, C.B. Fitzgerald, *Nature Mater.* **4**, 173 (2005).
- [4] C. Sudakar, J.S. Thakur, G. Lawes, R. Naik, V.M. Naik, *Phys. Rev. B* **75**, 054423 (2007).
- [5] T. Dietl, *Acta Phys. Pol. A* **111**, 27 (2007).
- [6] U. Narkiewicz, D. Sibera, I. Kuryliszyn-Kudelska, L. Kilanski, W. Dobrowolski, N. Romcevic, *Acta Phys. Pol. A* **113**, 1695 (2008).
- [7] A.L. Patterson, *Phys. Rev.* **56**, 978 (1939).
- [8] N. Ashkenov, B.N. Mbenkum, C. Bundesmann, V. Riede, M. Lorenz, D. Spemann, E.M. Kaidashev, A. Kasic, M. Shubert, M. Grundmann, *J. Appl. Phys.* **93**, 126 (2003).
- [9] E.F. Venger, A.V. Melnichuk, L.Lu. Melnichuk, Yu.A. Pasechuk, *Phys. Status Solidi B* **188**, 823 (1995).
- [10] Z. Wang, D. Schiferl, Y. Zhao, H.St. C. O'Neill, *J. Phys. Chem. Solids* **64**, 2517 (2003).
- [11] F. Bauciuman, F. Patcas, R. Craciun, D.R.T. Zahn, *Phys. Chem. Chem. Phys.* **1**, 185 (1999).
- [12] O.N. Shebanova, P. Lazar, *J. Solid State Chem.* **174**, 424 (2003).
- [13] V.G. Hajdiev, M.N. Iliev, I.V. Vergilov, *J. Phys. C, Solid State Phys.* **21**, 1199 (1988).